Electron tunneling in a strained n-type Si1−xGex/Si/Si1−xGex double-barrier structure

K. M. Hung
National Kaohsiung University of Applied Sciences

T. H. Cheng
National Taiwan University

W. P. Huang
National Taiwan University

K. Y. Wang
National Taiwan University

H. H. Cheng
National Taiwan University

See next page for additional authors

Authors
K. M. Hung, T. H. Cheng, W. P. Huang, K. Y. Wang, H. H. Cheng, Greg Sun, and R. A. Soref

AIP Applied Physics Letters

Electron tunneling in a strained n-type Si1−xGex/Si/Si1−xGex double-barrier structure

K. M. Hung, T. H. Cheng, W. P. Huang, K. Y. Wang, H. H. Cheng et al.

Citation: Appl. Phys. Lett. **93**, 123509 (2008); doi: 10.1063/1.2991295
View online: http://dx.doi.org/10.1063/1.2991295
View Table of Contents: http://apl.aip.org/resource/1/APPLAB/v93/i12
Published by the American Institute of Physics.

Electron tunneling in a strained n-type $Si_{1-x}Ge_x/Si/Si_{1-x}Ge_x$ double-barrier structure

K. M. Hung,[1] T. H. Cheng,[2] W. P. Huang,[2] K. Y. Wang,[2] H. H. Cheng,[2,a)] G. Sun,[3] and R. A. Soref[4]
[1]*Department of Electronics Engineering, National Kaohsiung University of Applied Sciences, Kaohsiung 807, Taiwan*
[2]*Center for Condensed Matter Sciences and Graduate Institute of Electronics Engineering, National Taiwan University, Taipei 106, Taiwan*
[3]*Department of Physics, University of Massachusetts–Boston, Boston, Massachusetts 02125, USA*
[4]*Air Force Research Laboratory, Sensors Directorate, Hanscom AFB, Massachusetts 01731, USA*

(Received 5 June 2008; accepted 5 September 2008; published online 26 September 2008)

We report electrical measurements on an n-type $Si_{1-x}Ge_x/Si/Si_{1-x}Ge_x$ double-barrier structure grown on a partially relaxed $Si_{1-y}Ge_y$ buffer layer. Resonance tunneling of Δ_4 band electrons is demonstrated. This is attributed to the strain splitting in the SiGe buffer layer where the Δ_4 band is lowest in energy at the electrode. Since the Δ_4 band electrons have a much lighter effective mass along the direction of tunneling current in comparison with that of the Δ_2 band electrons, this work presents an advantage over those SiGe resonant-tunneling diodes in which tunneling of Δ_2 band electrons is employed. © *2008 American Institute of Physics*. [DOI: 10.1063/1.2991295]

Strained Si grown upon a relaxed $Si_{1-x}Ge_x$ buffer layer is a basic building element for high-speed Si-based electronic devices.[1–3] With strain, both the conduction and valence band edges split. Therefore, understanding the electrical properties of $Si_{1-x}Ge_x/Si$ heterostructures under different strain situations is important in optimizing various electrical and optical devices made of such structures. However, due to the small conduction band (CB) offset between Si and $Si_{1-x}Ge_x$, the electrical characteristics of n-type $Si/Si_{1-x}Ge_x$ structures have not been thoroughly investigated. A previous study reported the observation of resonant tunneling in a double barrier $Si_{1-x}Ge_x/Si/Si_{1-x}Ge_x$ structure grown on a relaxed $Si_{1-y}Ge_y$ buffer layer,[4] where a single feature can be associated with the resonance tunneling of Δ_2 band electrons. In this paper, we present current-voltage (I-V) measurement results that reveal two features of resonance tunneling in a double barrier $Si_{1-x}Ge_x/Si/Si_{1-x}Ge_x$ structure wherein strain is distributed in both the Si and $Si_{1-x}Ge_x$ layers. With the analysis of strain-induced band splitting and the theoretical modeling of the electrical characteristic, we show that these features are dominated by the resonance tunneling of Δ_4-band electrons, which have lighter effective mass along the direction of tunneling than the Δ_2-band electrons. Since the Δ_4 band can form a spatially direct type-I band alignment (still indirect in k-space) in $Si/Si_{1-x}Ge_x$ heterostructures with proper strain manipulation,[5] this work should have an impact on electronic as well as optical applications of $Si_{1-x}Ge_x/Si$ heterostructure devices.

The $Si_{0.45}Ge_{0.55}/Si/Si_{0.45}Ge_{0.55}$ double-barrier structure used in this study was grown by molecular beam epitaxy on a p-type Si (001) wafer. Our structure consists of (a) a layer of Si (1000 Å) grown at low temperature, (b) a buffer layer of $Si_{0.83}Ge_{0.17}$ (3000 Å), (c) a 1500 Å of $Si_{0.83}Ge_{0.17}$ with n-type Sb doping, (d) a 200 Å Si spacer layer, (e) a 45 Å $Si_{0.45}Ge_{0.55}$ barrier layer, (f) a 58 Å Si quantum well (QW) layer, (g) a 45 Å $Si_{0.45}Ge_{0.55}$ barrier layer, (h) a 200 Å Si spacer layer, and (i) a 1500 Å of $Si_{0.83}Ge_{0.17}$ with n-type Sb doping. Layer (a) is grown at 430 °C while 600 °C growth is used for the other layers. Layers (c) and (i) are lightly doped with a nominal concentration of 1×10^{17} cm^{-3}. The alloy compositions were determined by high resolution x-ray diffraction measurement, and the layer thicknesses are measured by cross-section transmission electron microscopy (TEM). The structural image is shown in Fig. 1 and the micrograph of the QW region is shown in the inset indicating a small thickness fluctuation in the QW region but high quality overall. A partially relaxed buffer layer is fabricated by employing a previously developed growth technique. Si and $Si_{0.45}Ge_{0.55}$ layers in the QW region experience different strains.[6,7] The strain in different layers was determined by Raman measurement, and it is found that (a) the buffer layer is partially relaxed with in-plane strain of $\varepsilon_{\parallel}=-0.23\%$ and (b) in the QW region, the strain in Si ($Si_{0.45}Ge_{0.55}$) layer is

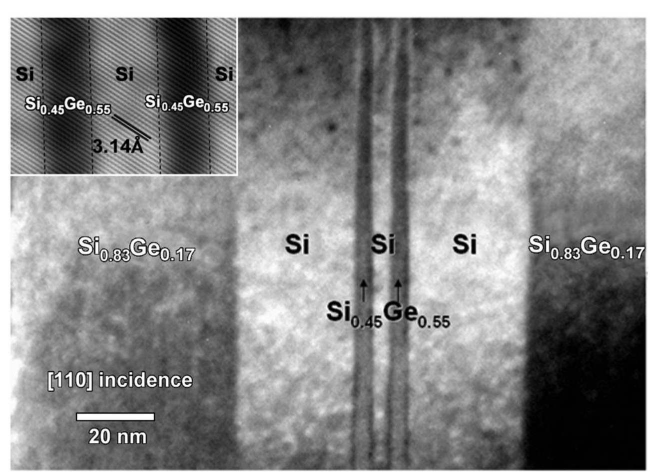

FIG. 1. (a) TEM image of the $Si_{0.45}Ge_{0.55}/Si/Si_{0.45}Ge_{0.55}$ double barrier structure with an inset showing the micrograph of the double barrier QW region.

a)Author to whom correspondence should be addressed. Electronic mail: hhcheng@ntu.edu.tw.

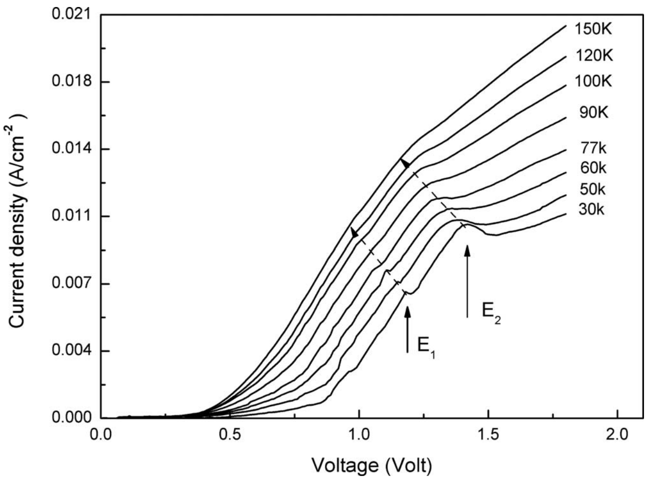

FIG. 2. *I-V* characteristics measured in the temperature range from 30 to 150 K.

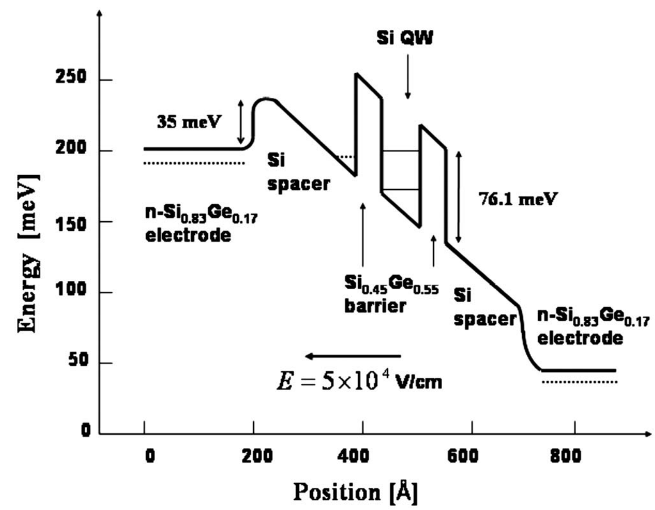

FIG. 3. Δ_4 band alignment of the $Si_{0.45}Ge_{0.55}/Si/Si_{0.45}Ge_{0.55}$ double barrier structure under the bias that produced an electric field of 5×10^4 V/cm. The dotted lines indicate the positions of quasi-Fermi levels in different regions.

$\varepsilon_{\parallel}=0.403\%(-1.7\%)$, where the positive (minus) sign indicates tensile (compressive) strain.

The *n-i-n* structure is fabricated into a mesa structure with a top contact area of 75×75 μm^2, and Ohmic contacts are formed by depositing a thin layer of Cr followed by Au evaporation. *I-V* measurement is performed using Keithley 236 source meter within the temperature range of 30–150 K. Below 30 K, we were unable to obtain an electrical signal because of the relatively low doping and issues with the frozen contacts. Above 150 K, the characteristic of tunneling is less profound due to thermal effects.

Temperature dependent *I-V* curves are plotted in Fig. 2. We first discuss the electrical characteristic obtained at 30 K. At low applied voltage $V_{\text{bias}}<0.5$ V, the current is negligible when there are little electrons accumulated in the Si spacer to tunnel through the double barrier. As the applied voltage increases, we can clearly resolve two features of resonance tunneling as marked by the solid arrow lines: one is located at $V_{\text{bias}}(E_1)=1.18$ V (labeled E_1) and the other at $V_{\text{bias}}(E_2)=1.42$ V (labeled E_2). The current densities of these two sharp features are 10.25 mA/cm^2 (E_1) and 9.68 mA/cm^2 (E_2) with a peak-to-valley ratio of 1.02 and 1.06, respectively. These features can be attributed to resonance tunneling when the Fermi energy at the injection electrode lines up with one of the confined states in the QW. As the applied bias continues to increase, the band profile is further tilted to move the Fermi level from one confined state to the next. As the temperature increases, the positions of these features shift and become broader with decreasing peak-to-valley ratio due to thermal broadening of energy levels at both the electrode and the QW region as indicated by the dashed arrow lines.

We subsequently performed theoretical analysis in order to gain insight into the origin of these tunneling features. In the absence of strain, the CB edge of the Si lies below that of the $Si_{1-x}Ge_x$ layer.[8] When strain is present, the sixfold degeneracy of the band edge is lifted and splits into Δ_2 and Δ_4 bands with an energy separation of Ξe_T, where Ξ is the deformation potential of the material and e_T is the lattice mismatch.[8] Under compressive strain, the Δ_4 band edge falls in energy at a rate of $\Xi e_T/3$, while for the Δ_2 band, the band edge rises in energy at a rate of $2\Xi e_T/3$. Using the parameters from Refs. 5 and 9 and the measured values for strain, we calculated Δ_2- and Δ_4-band offsets between the different regions. The CB offsets in the QW region are 276.4 and 76.1 meV for Δ_2 and Δ_4 bands, respectively. Since the contact electrode $Si_{0.83}Ge_{0.17}$ layer experiences compressive strain, its Δ_4 band forms the lowest energy states. The transport behavior should thus be dominated by Δ_4-band electrons. In Fig. 3, we have plotted the Δ_4-band alignment under the applied bias that produced an electric field of 5×10^4 V/cm. With this band profile, we can now calculate the confined states of electrons by solving the Schrödinger equation. There are two confined Δ_4-band states as shown in Fig. 3.

The electron transport can be divided into two sequential processes. First, under bias electrons are injected into the Si spacer region through the small energy barrier of 35 meV by either tunneling or thermionic emission. Second, the electrons accumulated in the spacer tunnel through the double barrier region to reach the opposite side of the structure. The relationship between the two processes is such that the first process injects electrons into the spacer region, which causes the quasi-Fermi level in Si spacer to increase, and when this Fermi level lines up with one of the confined states in the QW, the resonance tunneling appears. The current in these two sequential processes should be limited by the resonance tunneling of the QW region. Thus, the quasi-Fermi level in the Si spacer region should almost be lined up with the Fermi level in the doped $Si_{0.83}Ge_{0.17}$ region on the left (dotted lines in Fig. 3). Assuming a uniform electric field distribution in the spacer-barrier-well-barrier-spacer region, we have then calculated the tunneling current as a function of the bias voltage according to[10]

$$J=\frac{em_{t,\Delta_{2,4}}k_BT}{2\pi^2\hbar^3}\int T_{\Delta_{2,4}}(E)\ln\frac{1+\exp[(E_f-E)/k_BT]}{1+\exp[(E_f-eV_{\text{bias}}-E)/k_BT]}dE, \quad (1)$$

where T is the temperature, E_f is the Fermi level of the electrode, $m_{t,\Delta_{2,4}}$ is the electron effective mass along the tunneling direction, and $T_{\Delta_{2,4}}(E)$ is the energy dependent transmission coefficient for either Δ_2- or Δ_4-band electrons and can be obtained by the transfer matrix technique, which

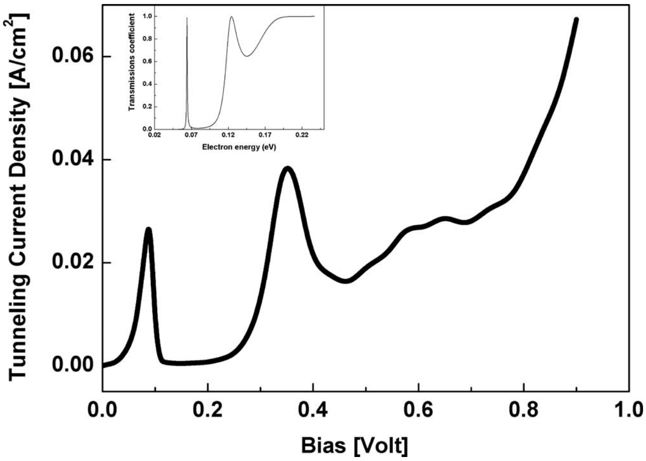

FIG. 4. Tunneling current calculated as a function of applied bias with an inset showing the energy-dependent transmission coefficient at the zero bias.

treated the tiled potential profile with a piecewise steplike function.[11] The calculated result of tunneling current for the Δ_4-band electrons with $m_{t,\Delta_4}=0.19m_o$ is shown in Fig. 4, where two peaks associated with the resonance tunneling are located at the bias voltages of $V_1=0.09$ V and $V_2=0.35$ V. (T_{Δ_4} at zero bias is also shown in the inset of Fig. 4.) In comparison with the measurement, the tunneling currents agree within the same order of magnitude, but the calculated peak positions are consistently less than the measured values in voltage. This discrepancy can be attributed to the parasitic series resistance in the contact regions and can be reduced by comparing the voltage differences of these resonance positions. The agreement between the measurement $V_{\text{bias}}(E_2)-V_{\text{bias}}(E_1)=0.22$ V and the calculation $V_2-V_1=0.26$ V is indeed much better. The rather small discrepancy can be accounted for by the different current values at resonance and the thickness fluctuation in the QW region as shown in the TEM micrograph (inset of Fig. 1). In comparison with that of Δ_4-band electrons, the tunneling current of Δ_2-band electrons is much smaller because the profile of T_{Δ_2} is considerably narrower due to the larger Δ_2-band barrier height and heavier effective mass ($m_{t,\Delta_2}=0.92m_o$) along the tunneling direction.[10] (The integral in Eq. (1) over the narrow profile of T_{Δ_2} is negligible).

In comparison with the previous investigation where Δ_2-band electron tunneling is observed,[4] the demonstration of Δ_4-band electron tunneling in our sample arises from the fact that the buffer layer, which serves as the electrode in our measurement, is partially relaxed. This is in contrast to the fully relaxed buffer layer used in the former study,[4] which produced tensile strain in the Si spacer layer grown on top resulting in Δ_2 band forming the lowest states. The partially strained buffer layer in our sample creates a desirable situation wherein the Δ_4 band forms the lowest energy states, which have a much lighter effective mass along the tunneling direction, yielding a larger tunneling current.

Financial support from the National Science Council, Taiwan (Grant Nos. NSC 95-2112-M-002-050 and NSC 97-2112-M-151-001-MY3) and AFOSR (USA) is gratefully acknowledged.

[1]R. A. Soref, Proc. IEEE **81**, 1687 (1993).
[2]P. M. Mooney and J. O. Chu, Annu. Rev. Mater. Sci. **30**, 335 (2000).
[3]M. L. Lee, E. A. Fitzgerald, M. T. Bulsara, M. T. Currie, and A. Lochtefeld, J. Appl. Phys. **97**, 011101 (2005).
[4]D. J. Paul, P. Lee, I. V. Zozoulenko, K.-F. Berggren, B. Kabius, B. Holländer, and S. Mantl, Appl. Phys. Lett. **91**, 072108 (2000).
[5]K. Y. Wang, W. P. Huang, H. H. Cheng, G. Sun, R. A. Soref, R. J. Nicholas, and Y. W. Suen, Appl. Phys. Lett. **91**, 072108 (2007).
[6]W. S. Tan, H. H. Cheng, V. I. Mashanov, Y. F. Wong, and C.-T. Chia, Appl. Phys. Lett. **88**, 162111 (2006).
[7]W. P. Huang, H. H. Cheng, G. Sun, R. F. Lou, J. H. Yeh, and T. M. Shen, Appl. Phys. Lett. **91**, 142012 (2007).
[8]R. People, Phys. Rev. B **32**, 1405 (1985).
[9]H. H. Cheng, S. T. Yen, and R. J. Nicholas, Phys. Rev. B **62**, 4638 (2000).
[10]K. M. Hung and G. Y. Wu, Phys. Rev. B **45**, 3461 (1992).
[11]P. Harrison, *Quantum Wells, Wires and Dots* (Wiley, New York, 2002), p. 62.